5.5 ADVANTAGES OF THE D'ALEMBERT METHOD. THE GYRO

As the preceding examples demonstrate, there are sometimes two advantages to the D'Alembert approach when systems of rigid bodies are involved:

(1) The procedure is *more systematic* because inertial forces are cast in the same form as spring forces and friction forces, and need no special treatment.

(2) The procedure is *more versatile*, and therefore *more efficient*, because (a) free-body diagrams can be drawn of *systems* of rigid bodies taken together, so that internal forces need not be considered, and (b) moments can be taken about any axis.

In addition, physical intuition is reinforced by the concept of inertial reaction forces opposing acceleration whenever it tries to occur.

For these reasons the D'Alembert approach (5.35), (5.36) will be used for most of the examples in this book. But the reader will certainly find little difficulty in substituting a Newtonian derivation whenever he chooses.

We submit one further, rather advanced example, in which rotating reference frames play a helpful role. (Refer again to Sec. 5.2.)

Example 5.7. The two-axis gyro. Gyros for sensing angular motion are the heart of airplane automatic pilots, rocket-vehicle launch-guidance systems, space-vehicle attitude-control systems, ship's gyrocompasses, and submarine inertial autonavigators. A physical model for a typical gyro instrument is shown in Fig. 5.8. The rotor is driven at constant speed n with respect to inner gimbal g.

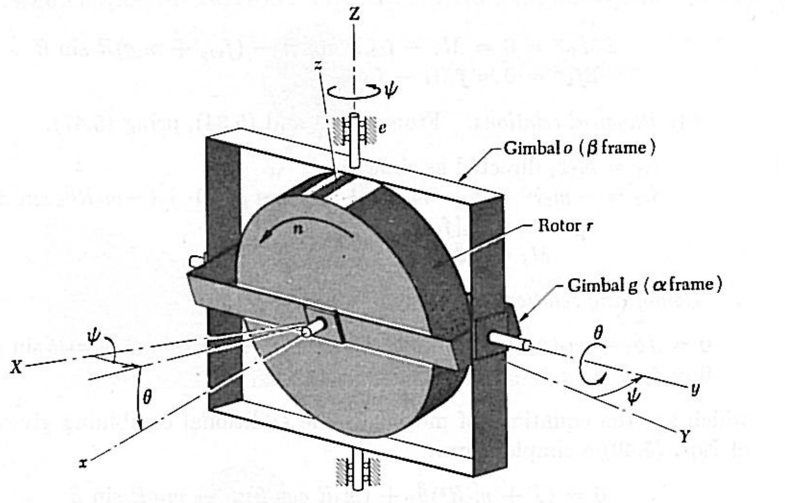

(a) *System in an arbitrary configuration*

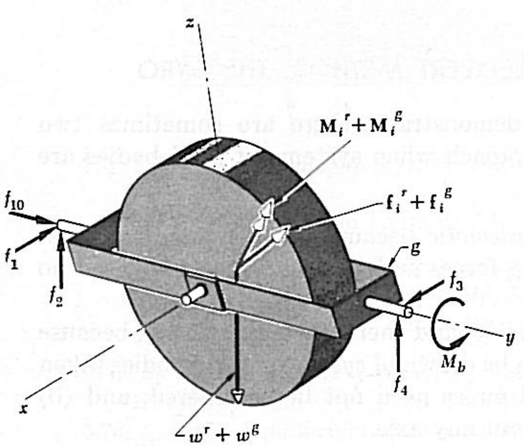

(b) *Free-body diagram of rotor r plus gimbal g*

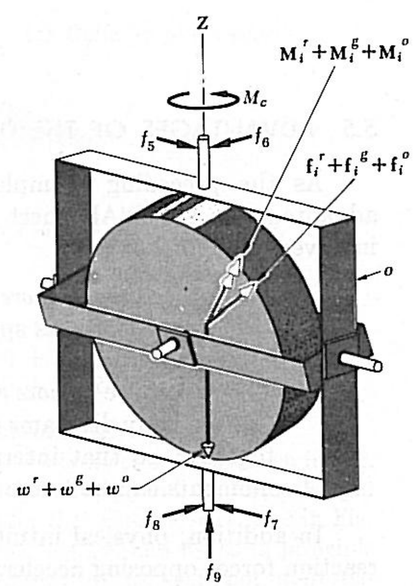

(c) *Free-body diagram of rotor r plus gimbal g plus gimbal o*

Fig. 5.8 *Two-axis gyro*

Angle θ defines the angular position of the inner gimbal g with respect to the outer gimbal o; and angle ψ defines the angular position of the outer gimbal with respect to the earth e (or with respect to the vehicle to which the gyro is mounted). (Gimbal angles θ and ψ are measured with electrical pickoffs in many applications.)

Derive the equations of motion for study of rapid transient motions of the system.

To further define the *physical model* (Stage I) we assume that the rotor is

perfectly balanced and symmetrical, and that the bearings are rigid and perfectly centered. We assume that a moment M_b is exerted about the y axis, between gimbals g and o, and that a moment M_c is exerted about the Z axis on the outer gimbal by the fixed base. In this analysis of high-speed transient motions of the rotor we take the earth (or vehicle) to be an inertially fixed reference.†

To derive the *equations of motion* (Stage II) we follow Procedure A-m, p. 35.

(1) *Geometry.* Figure 5.8*a* shows the system in an arbitrary configuration (with respect to fixed reference XYZ), and coordinates θ and ψ are defined. The system has two degrees of freedom (the speed n of the rotor with respect to gimbal g being prescribed as constant).

It will be convenient to employ both the α reference frame (fixed in the inner gimbal g) and the β frame (fixed in the outer gimbal o). The angular velocities of these frames are [using (5.11)]

$$\mathbf{\Omega}^\beta = \mathbf{1}_Z\dot{\psi} \tag{5.50}$$

$$\begin{aligned}\mathbf{\Omega}^\alpha &= \mathbf{\Omega}^{\alpha/\beta} + \mathbf{\Omega}^\beta \\ &= \mathbf{1}_y(\dot{\theta}) + \mathbf{1}_Z(\dot{\psi})\end{aligned}$$

or

$$\mathbf{\Omega}^\alpha = \mathbf{1}_x(-\dot{\psi}s\theta) + \mathbf{1}_y(\dot{\theta}) + \mathbf{1}_z(\dot{\psi}c\theta) \tag{5.51}$$

in which the last expression is obtained by decomposing $\mathbf{1}_Z\dot{\psi}$ into its components along the x and z axes, the shorthand $s\theta \triangleq \sin\theta$ and $c\theta \triangleq \cos\theta$ being employed. Finally, the angular velocity of the rotor is

$$\begin{aligned}\mathbf{\Omega}^r &= \mathbf{\Omega}^{r/\alpha} + \mathbf{\Omega}^\alpha \\ &= \mathbf{1}_x n + \mathbf{1}_y\dot{\theta} + \mathbf{1}_Z\dot{\psi}\end{aligned}$$

or

$$\mathbf{\Omega}^r = \mathbf{1}_x(n - \dot{\psi}s\theta) + \mathbf{1}_y(\dot{\theta}) + \mathbf{1}_z(\dot{\psi}c\theta) \tag{5.52}$$

(2) *Force equilibrium.* (i) Select subsystems. Since there are only two independent variables, θ and ψ, we expect that two equations of motion will be sufficient to describe the motion. The key to writing them directly is the shrewd choice of free bodies. The pair of free-body diagrams which do the job are shown in Fig. 5.8*b*, the rotor plus inner gimbal, and 5.8*c*, the entire system.

(ii) Write force-balance equations. For the free-body diagram of Fig. 5.8*b* there is just one equilibrium equation that can be written which does not involve the bearing forces $f_1, \ldots, f_4$, and that is Eq. (5.36) written about the y axis:

$$\text{System } g + r \qquad (\Sigma\mathbf{M}^*)_y = 0 = (\mathbf{M}_i^r + \mathbf{M}_i^g)_y + M_b \tag{5.53}$$

(Note that the assumption of perfect balance in Stage I implies that each of the forces $\mathbf{f}_i^r$, $\mathbf{f}_i^g$, w^r, w^g, has zero moment about the y axis.)

Similarly, for the free-body diagram of Fig. 5.8*c* there is just one equilibrium equation that can be written which does not involve the bearing forces $f_5, \ldots, f_8$, and that is Eq. (5.36) written about the Z axis:

$$\text{System } g + r + o \qquad (\Sigma\mathbf{M}^*)_Z = 0 = (\mathbf{M}_i^r + \mathbf{M}_i^g + \mathbf{M}_i^o)_Z + M_c \tag{5.54}$$

† By contrast, if we were interested in analyzing the gyro as a gyrocompass, the motion of the earth would, of course, be of primary importance.

which is more convenient to write in the form

$$0 = (\mathbf{M}_i{}^r + \mathbf{M}_i{}^g)_z \cos\theta - (\mathbf{M}_i{}^r + \mathbf{M}_i{}^g)_x \sin\theta + (\mathbf{M}_i{}^o)_Z + M_c \tag{5.55}$$

as we shall see.

(3) *Physical relations.* Using (5.37) and (5.16), we can write expressions for the inertial moments $\mathbf{M}_i$, shown in the free-body diagrams of Fig. 5.8*b* and *c*:

$$\begin{aligned} -\mathbf{M}_i{}^r &= \dot{\mathbf{H}}^r = \overset{\alpha}{\dot{\mathbf{H}}}{}^r + \mathbf{\Omega}^\alpha \times \mathbf{H}^r \\ -\mathbf{M}_i{}^g &= \dot{\mathbf{H}}^g = \overset{\alpha}{\dot{\mathbf{H}}}{}^g + \mathbf{\Omega}^\alpha \times \mathbf{H}^g \\ -\mathbf{M}_i{}^o &= \dot{\mathbf{H}}^o = \overset{\beta}{\dot{\mathbf{H}}}{}^o + \mathbf{\Omega}^\beta \times \mathbf{H}^o \end{aligned} \tag{5.56}$$

in which differentiation in the α and β frames, respectively, has been selected because $\mathbf{H}^r$ and $\mathbf{H}^g$ are most simply expressed in the α frame (in which their moments of inertia are constant), while $\mathbf{H}^o$ is most simply expressed in the β frame (in which its moments of inertia are constant). Axes x, y, z, are (by symmetry) principal axes of both r and g, and thus, using (5.38), (5.52), and (5.51), we obtain

$$\left.\begin{aligned} \mathbf{H}^r &= \mathbf{1}_x[J_x{}^r(n - \dot\psi s\theta)] + \mathbf{1}_y[J_y{}^r\dot\theta] + \mathbf{1}_z[J_z{}^r\dot\psi c\theta] \\ \mathbf{H}^g &= \mathbf{1}_x[J_x{}^g(-\dot\psi s\theta)] \quad + \mathbf{1}_y[J_y{}^g\dot\theta] + \mathbf{1}_z[J_z{}^g\dot\psi c\theta] \\ &\text{Similarly, } Z \text{ is a principal axis for } o\text{:} \\ \mathbf{H}^o &= \mathbf{1}_Z[J_Z{}^o\dot\psi] \end{aligned}\right\} \tag{5.57}$$

We define the following, for convenience in handling the nomenclature:

$h \triangleq J_x{}^r n$ (this is the rotor's constant "spin momentum" with respect to the gimbal g)

$$J_x \triangleq J_x{}^r + J_x{}^g \qquad J_y \triangleq J_y{}^r + J_y{}^g \qquad J_z \triangleq J_z{}^r + J_z{}^g$$

Then, substituting (5.57) into (5.56), and computing only the components required by (5.53) and (5.55), gives

$$-(\mathbf{M}_i{}^r + \mathbf{M}_i{}^g)_y = J_y\ddot\theta + h\dot\psi\cos\theta + (J_z - J_x)\dot\psi^2 \sin\theta\cos\theta \tag{5.58}$$

$$\begin{aligned} -(\mathbf{M}_i{}^r + \mathbf{M}_i{}^g)_z \cos\theta &= J_z(\ddot\psi\cos^2\theta - \dot\psi\dot\theta\sin\theta\cos\theta) - h\dot\theta\cos\theta \\ &\quad + (J_x - J_y)\dot\psi\dot\theta\sin\theta\cos\theta \end{aligned} \tag{5.59}$$

$$\begin{aligned} -(\mathbf{M}_i{}^r + \mathbf{M}_i{}^g)_x \sin\theta &= -J_x(\ddot\psi\sin^2\theta + \dot\psi\dot\theta\cos\theta\sin\theta) \\ &\quad + (J_z - J_y)\dot\psi\dot\theta\cos\theta\sin\theta \end{aligned} \tag{5.60}$$

Combine terms. Substituting (5.58), (5.59), and (5.60) into (5.53) and (5.55), respectively, as required, gives:

$$J_y\ddot\theta + h\dot\psi\cos\theta + (J_z - J_x)\dot\psi^2\sin\theta\cos\theta = M_b \tag{5.61}$$

$$\begin{aligned} (J_Z{}^o + J_z\cos^2\theta + J_x\sin^2\theta)\ddot\psi &- h\dot\theta\cos\theta \\ &+ 2(J_x - J_z)\dot\psi\dot\theta\sin\theta\cos\theta = M_c \end{aligned} \tag{5.62}$$

which are the exact equations of motion for the ideal two-axis gyro.

Linear approximation for small motions. In many applications of interest it may be assumed that the motions ψ and θ will be very small (the order of milliradians or arc seconds). Further, the spin speed n will be large compared to $\dot\psi$. This permits dropping the $J\dot\psi^2\sin\theta$ and $J\dot\psi\dot\theta\sin\theta$ terms in (5.61)

and (5.62), compared with the terms in $h\dot\psi = Jn\dot\psi$ and $h\dot\theta = Jn\dot\theta$. Then, using the usual small-angle approximations, $\sin\theta = \theta$ and $\cos\theta = 1$, we obtain the following linear equations:

Two-axis gyro equations for small motions

$$\boxed{\begin{aligned} J_y\ddot\theta + h\dot\psi &= M_b \\ J_Z\ddot\psi - h\dot\theta &= M_c \end{aligned}} \qquad \begin{aligned} &(5.63) \\ &(5.64) \end{aligned}$$

in which $J_Z \triangleq J_Z{}^o + J_z$. These linear equations for a two-axis gyro are very useful in making linear calculations of gyro behavior, as we shall demonstrate in Sec. 19.5. Usually M_b and M_c are made as small as possible (very good bearings are used), and consist primarily of light viscous damping, $M_b = -b\dot\theta$, and $M_c = -c\dot\psi$.

The single-axis gyro. In many gyro applications the outer gimbal is fastened rigidly to a vehicle. Then only the inner gimbal is free to move, and the instrument is called a single-axis gyro. For this instrument, only Eq. (5.63) is required, the motion of ψ now being a prescribed input motion:

$$J_y\ddot\theta = M_b - h\dot\psi \tag{5.65}$$

Several versions of the single-axis gyro can be made, depending on the arrangements made for M_b. For example, if a spring and viscous damper are provided, so that $M_b = -k\theta - b\dot\theta + M_u$ (refer again to Fig. 5.8*a*), then the resulting instrument is called a *rate gyro*, and has the equation of motion:

Single-axis gyro

$$\boxed{J\ddot\theta + b\dot\theta + k\theta = -h\dot\psi + M_u} \tag{5.66}$$

in which M_u is uncertainty torque due to unbalance, stray magnetic field, and other causes. An actual single-axis gyro is shown in Fig. 19.13*a*.

Versions of the single-axis gyro will be studied in Problems 19.18 and 19.19.

Problems 5.69 through 5.70

19.5 THE TWO-AXIS GYROSCOPE

Few devices have dynamic behavior as intriguing as that of the two-axis gyroscope. Moreover, the device is of great practical modern interest as a sensor in control and guidance systems for air, sea, and space vehicles.

Gyroscopes, or gyros, as they are more commonly called, come in many forms and sizes. One common arrangement is shown in Fig. 19.10*a*, where the gyro rotor is mounted to the vehicle frame via two gimbals in such a way that the vehicle and rotor can move freely through small angles about any axis without exerting any torque on one another. In other forms the gyro rotor may be spun about a spherical bearing, giving it the same complete freedom from angular motion of the vehicle; or the rotor may itself be a sphere which is supported electrically, magnetically, or by gas film, so as to be free rotationally from the vehicle.

The usual application of the free gyro is as a directional reference. The spinning mass has, as we shall show presently, an extremely strong tendency to maintain its spin direction in space. When it is supported free of the vehicle (as described above), it therefore continues to point in a fixed spatial direction despite rotation of the vehicle around it. But a free gyro may have interesting dynamic motions of its own, independent of the vehicle, and it is these we wish to study here. We use the configuration of Fig. 19.10*a* because a convenient coordinate system is defined by the gimbals, making it particularly easy to keep track of what is happening.

In this study, then, let us *compute the time response of the free gyro of Fig.* 19.10*a following initial conditions* (*displacement and velocity*), *and also the response resulting from an impulsive- or a step-disturbance torque on the gimbals,* the base being held fixed throughout.

STAGE I. PHYSICAL MODEL. Assume in this first analysis that in Fig. 19.10*a* the axially symmetrical rotor is carefully mounted so that its spin axis is its major axis of inertia. Assume also that the gimbals are carefully balanced, that the rotor is driven at constant speed with respect to the inner gimbal by a precision motor, and that damping in the gimbal bearings can be neglected. The effect of gravity acting on a gimbal unbalance will be considered explicitly as a steady disturbing torque on the gimbal. A study of the effect of damping is outlined in Problem 19.30. Finally, we make the influential assumption that only small angles are involved in the motion. This is essential if the equations of motion are to be linear. (The study of large-angle motions of a free gyro is an advanced topic.)

STAGE II. EQUATIONS OF MOTION. The equations of motion for the above physical model were derived in Example 5.7, p. 159. A brief review follows.

(1) *Geometry.* The system has two unconstrained degrees of freedom. In the arbitrary-configuration sketch of Fig. 19.10*a* the variables ψ and θ serve

to define the system configuration: ψ is rotation of gimbal o with respect to a fixed reference frame, and θ is rotation of gimbal g with respect to gimbal o. Both ψ and θ can be measured directly, e.g., using electrical gimbal potentiometers. Rotor speed n, with respect to gimbal g, is prescribed constant. (The rotor's position about its axle is of no concern when the rotor is assumed to have perfect axial symmetry.)

(2) *Equilibrium.* Two free-body diagrams are utilized, Fig. 19.10*b* and *c*. For system 1 we write (2.2) about axis y, and for system 2, about axis Z.

(3) *Physical relations.* These involve inertial moments of the form $M_i = J\ddot{\theta}$ and $M_i = h\dot{\theta}$, which are substituted into the equilibrium relations. The result, for small motions θ and ψ, and for $\dot{\theta} \ll n$ and $\dot{\psi} \ll n$, is the pair of equations (5.63) and (5.64):

$$J_y\ddot{\theta} + h\dot{\psi} = M_y \qquad (19.44)$$

[(5.63) repeated]

$$-h\dot{\theta} + J_Z\ddot{\psi} = M_Z \qquad (19.45)$$

[(5.64) repeated]

in which J_y is the moment of inertia of system 1 (Fig. 19.10*b*) about axis y, J_Z is the moment of inertia of system 2 (Fig. 19.10*c*) about axis Z,† and h is defined by $h = I_{rx}n$, where I_{rx} is the moment of inertia of the rotor about its axis of symmetry [refer to (2.7)].

STAGE III. DYNAMIC BEHAVIOR. We follow Procedure D-1.

Step 1. Laplace transform the equations of motion:

$$\begin{bmatrix} s^2 & \dfrac{h}{J_y}s \\ -\dfrac{h}{J_Z}s & s^2 \end{bmatrix}\begin{bmatrix} \Theta \\ \Psi \end{bmatrix} = \begin{bmatrix} \dfrac{M_y(s)}{J_y} + s\theta(0^-) + \dot{\theta}(0^-) + \dfrac{h}{J_y}\psi(0^-) \\ \dfrac{M_Z(s)}{J_Z} - \dfrac{h}{J_Z}\theta(0^-) + s\psi(0^-) + \dot{\psi}(0^-) \end{bmatrix} \qquad (19.46)$$

Step 2. Manipulate algebraically to obtain:

(*b*) *Natural behavior.* The characteristic equation is given, from the left-hand side of (19.46), by

$$s^2\left(s^2 + \frac{h^2}{J_yJ_Z}\right) = 0 \qquad (19.47)$$

the roots of which are $s = 0, 0$, and $s = \pm jh/\sqrt{J_yJ_Z}$. The zero roots imply two natural "motions" in which the motion is a constant. We shall soon see that these are a constant displacement θ and a constant displacement ψ. The imaginary roots imply an oscillation at frequency $\omega = h/\sqrt{J_yJ_Z}$. To get an idea of the magnitude of ω, consider the limiting case that the gimbals are massless in Fig. 19.10*a*. Then J_y and J_Z are merely the diametral moments of inertia of the rotor disk, and they are equal to one-half its polar moment of inertia, $J_y = J_Z = I_{rx}/2$. Then, since $h = I_{rx}n$,

$$\omega = \frac{I_{rx}n}{\sqrt{I_{rx}^2/4}} = 2n \qquad (19.48)$$

† The small variation in J_Z with θ is second-order small, and is neglected in linear Eq. (19.46), as discussed in Example 5.7.

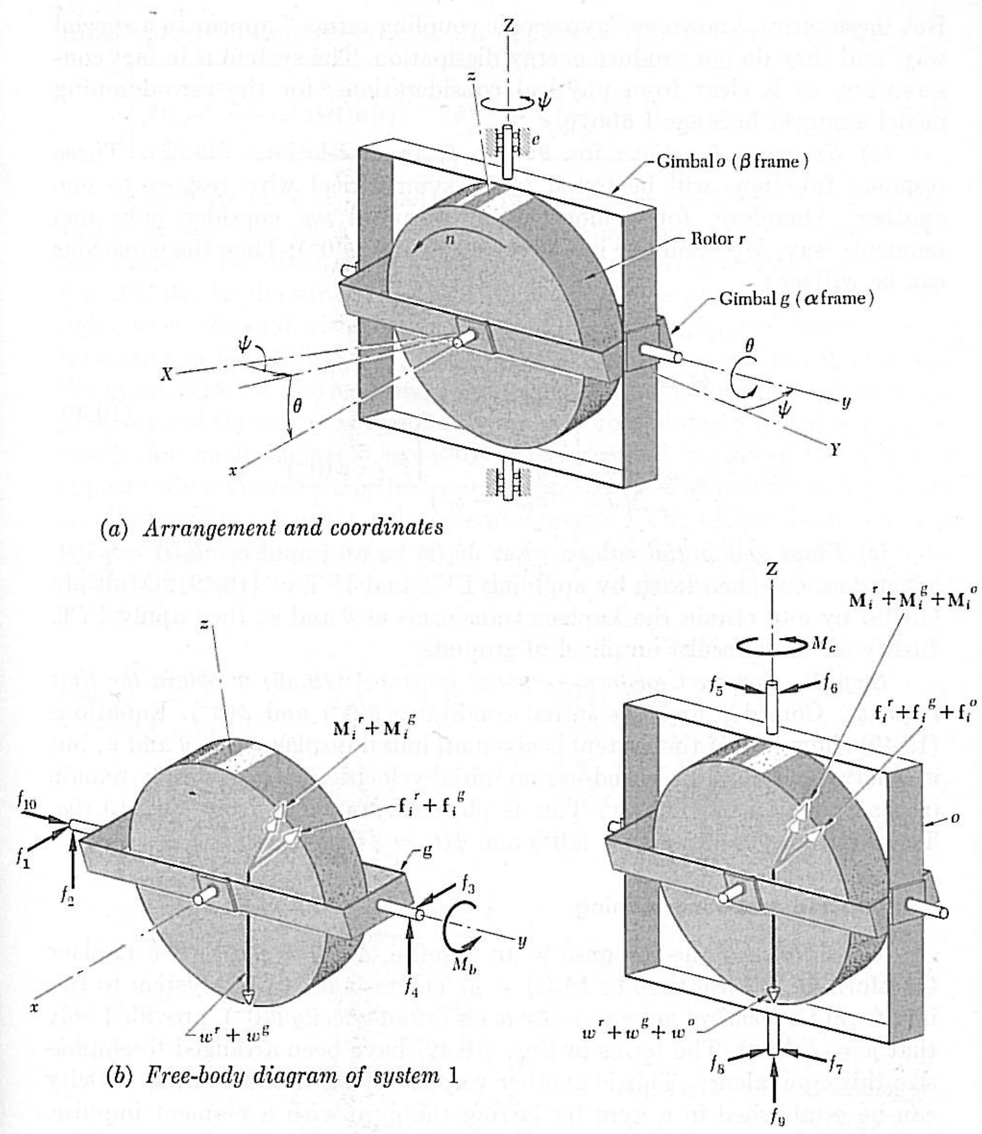

(*a*) *Arrangement and coordinates*

(*b*) *Free-body diagram of system 1*

Fig. 19.10 *The two-gimbal gyro*

(*c*) *Free-body diagram of system 2*

The oscillation frequency is twice the spin speed. Since real gimbals are not massless, a real gyro has an oscillation frequency somewhat less than $2n$—but typically of the same order of magnitude as n.

Another important point is evident from the characteristic equation: the oscillatory motion is undamped! This may be slightly surprising, since rate-dependent terms appear in both the equations of motion ($h\dot{\theta}$ and $h\dot{\psi}$).

But these terms, known as "gyroscopic coupling terms," appear in a special way, and they do not produce energy dissipation. The system is in fact conservative, as is clear from physical considerations, for the zero-damping model assumed in Stage I above.

(*a*) *Response functions* for θ and ψ, from relations (19.37). These response functions will be found to be symmetrical with respect to one another. Therefore, for demonstration purposes we consider only one moment—say, M_y—and one initial velocity—say, $\dot{\theta}(0^-)$. Then the equations can be written:

$$\Theta = \frac{\left[\dfrac{\mathsf{M}_y}{J_y} + \dot{\theta}(0^-)\right]}{s^2 + \omega^2} + \frac{\theta(0^-)}{s}$$
$$\Psi = \sqrt{\frac{J_y}{J_Z}}\,\frac{\left[\dfrac{\mathsf{M}_y}{J_y} + \dot{\theta}(0^-)\right]\omega}{s(s^2 + \omega^2)} + \frac{\psi(0^-)}{s} \qquad (19.49)$$

(*c*) *Final and initial values.* Let $M_y(t)$ be an impulse, $M_y(t) = \mu\delta(t)$. What does one then learn by applying FVT and IVT to (19.49)? Multiply (19.49) by s to obtain the Laplace transforms of $\dot{\theta}$ and $\dot{\psi}$; then apply IVT. Justify all these results on physical grounds.

Step 3. Inverse transform response functions (19.49) to obtain the time response. Consider first the initial conditions $\theta(0^-)$ and $\psi(0^-)$. Equations (19.49) show that if the system is given an initial displacement θ and ψ, but is otherwise undisturbed (and has no initial velocities), it will simply remain in that position indefinitely. This is physically obvious from Fig. 19.10*a*. That is, from (19.49), $\theta(t) = \theta(0^-)$ and $\psi(t) = \psi(0^-)$ for all $0 < t$.

Impulse response: coning

Consider next the response to an impulse, $M_y(t) = \mu\delta(t)$. The Laplace transform of M_y will then be $\mathsf{M}_y(s) = \mu$. The response of the system to this input will be *identical to its response to an initial velocity* $\dot{\theta}(0^-)$, provided only that $\mu = J_y\dot{\theta}(0^-)$. The terms in Eqs. (19.49) have been arranged to emphasize this equivalence. This is another way of saying that an initial velocity can be established in a gyro by jarring the gyro with a moment impulse. [Is this also borne out by the results of Step 2(*c*)?] Now let us see what motion follows. For simplicity, define the quantity Ω_{yo} by

$$\Omega_{yo} \triangleq \frac{\mu}{J_y} \qquad (19.50)$$

(Ω_{yo} is recognized as the initial velocity that μ will produce.) Then (19.49) becomes (for response to the impulse only)

$$\Theta = \frac{\Omega_{yo}}{s^2 + \omega^2} \qquad \Psi = \sqrt{\frac{J_y}{J_Z}}\,\Omega_{yo}\frac{\omega}{s(s^2 + \omega^2)} \qquad (19.51)$$

from which the time response to an impulse is (using, e.g., Table X)

$$\boxed{\theta(t) = \frac{\Omega_{yo}}{\omega}(\sin \omega t)u(t) \qquad \psi(t) = \sqrt{\frac{J_y}{J_Z}}\,\frac{\Omega_{yo}}{\omega}(1 - \cos \omega t)u(t)} \qquad (19.52)$$

A very useful way of plotting time response (19.52) is shown in Fig. 19.11. In one time plot, plot (*a*), $\theta(t)$ is plotted positive downward to correspond with the direction in which the spin axis moves when θ is positive in Fig. 19.10*a*. In the other time plot, plot (*b*), $\psi(t)$ is plotted positive to the right, to correspond with the direction in which the spin axis moves when ψ is positive in Fig. 19.10*a* (i.e., when the spin axis is viewed from the front of the gyro). Time is plotted downward in plot (*b*) for convenience. Now from plots (*a*) and (*b*) we can conveniently make a cross plot of θ versus ψ, plot (*c*), which (for small angles) is a picture of the way the motion of the spin axis appears when viewed from the front of Fig. 19.10*a*. The motion in Fig. 19.11 is called *coning*. (The spin axis generates a cone.) The reader should check a number of points on plot (*c*), which is drawn for J_Z slightly larger than J_y, and is elliptical. [Note from (19.52) that if $J_Z = J_y$ the path of the spin axis is circular.]

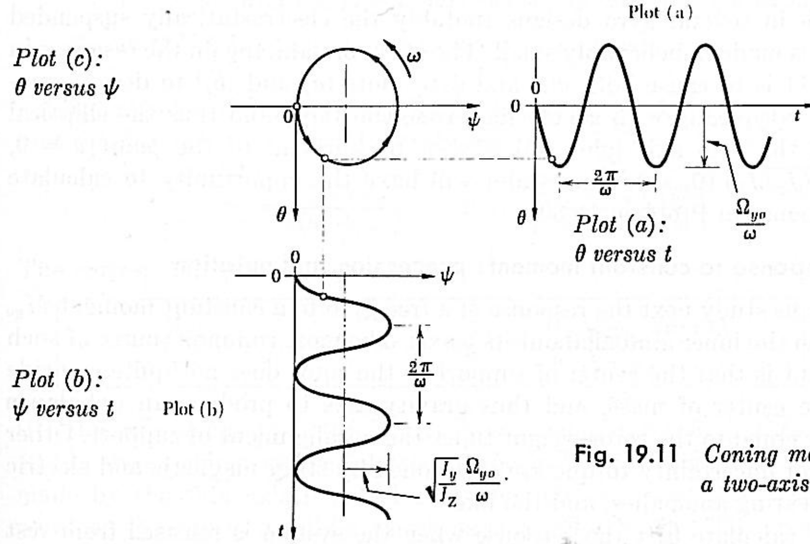

Fig. 19.11 *Coning motion of a two-axis gyro*

To get an idea of the import of this result, consider what the corresponding response to a moment impulse $\mu\delta(t)$ would be if the rotor were not spinning. Then, instead of tracing out the small ellipse of Fig. 19.11, plot (*c*), the spin axis would *tumble* about the y axis at velocity Ω_{yo}. Numerically, for example, suppose that the moments of inertia were

$$I_{rx} = 1000 \qquad J_y = 1200 \qquad J_Z = 1300$$

in cgs units [dn cm/(rad/sec), or gm cm²]. These represent a typical rotor of mass one-half kilogram. Then an impulse about y of

$$1000 \text{ dn cm sec} = 10^{-3} \text{ in. lb sec}$$

(one in. lb for 0.001 sec) would produce an Ω_{yo} of 0.83 rad/sec = 0.13 rev/sec. Next, suppose for comparison that the rotor is spinning at 2000 rad/sec (approximately 20,000 rpm) when the same impulse is applied. Then, instead of the spin axis *tumbling* at 0.13 revolution per second, its only motion will be a tiny coning motion of magnitude 0.52×10^{-3} rad. With typical instrument damping present, the *nonspinning* rotor will come to rest after perhaps a few *revolutions*, while the *spinning* rotor will move only half a *milliradian* (0.03 degree). The tremendous capability of a gyro to maintain its spatial orientation is thus dramatically demonstrated.

As the above calculations show, the coning motion of a typical instrument gyro is normally too small to be seen. Demonstration gyros have been developed which spin very slowly—e.g., at two or three revolutions per second (ω = 12 to 20). Then a large, slow coning motion can be produced with a reasonable impulse, and the results shown in Fig. 19.11 can readily be checked quantitatively.†

In almost any real gyro there will be some damping about both axes—although in several gyro designs (notably the electrostatically suspended gyro) it is made unbelievably small. The effect of damping on the response in Fig. 19.11 is to cause both $\theta(t)$ and $\psi(t)$ [plots (*a*) and (*b*)] to decay exponentially (typically with a very long time constant) and thus the elliptical path of the spin axis [plot (*c*)] is seen to spiral in to the point $\theta = 0$, $\psi = \sqrt{(J_y/J_Z)}\,(\Omega_{yo}/\omega)$. The reader will have the opportunity to calculate this response in Problem 19.30.

Response to constant moment: precession and nutation

Let us study next the response of a free gyro to a constant moment M_{yo} acting on the inner gimbal about its y axis. The most common source of such a moment is that the center of support of the rotor does not quite coincide with the center of mass, and thus gravity acts to produce an unbalance moment equal to the rotor weight times the misalignment of support. Other sources of uncertainty torque are occasioned by stray magnetic and electric fields, bearing anomalies, and the like.

We calculate first the response when the system is released from rest without initial conditions, but with the constant moment $M_y(t) = M_{yo}u(t)$

† A precisely known impulse can be applied to such a demonstration gyro in the following way: a known mass is tied to one end of a string; the other end of the string is tied to one end of the spin axle of the gyro. The mass is then released from a position at about the height of the axle and allowed to drop to the end of the string. It is caught on first bounce. It is found that the bounce velocity of the mass is negligible so that all of its linear momentum just before it reached the end of the string has been transferred as an impulse to the gyro; the magnitude of this impulse can be accurately calculated from the mass and the known drop height.

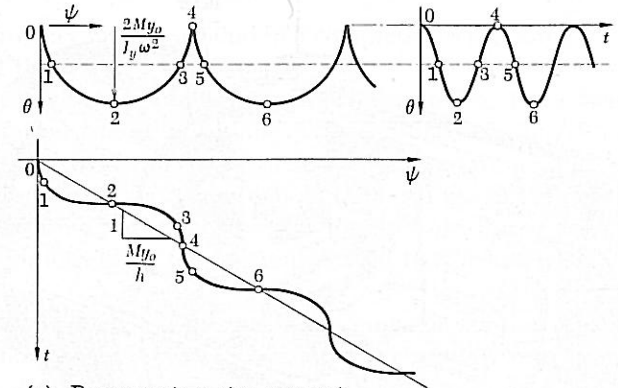

(*a*) *Response to a step moment*

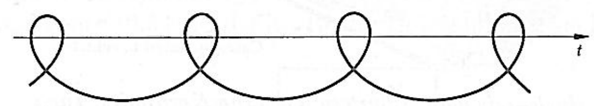

(*b*) *Response to a combination of step and impulse moment*

Fig. 19.12 *Precession and nutation of a two-axis gyro*

applied about the y axis. The Laplace transform of M_y is $\mathsf{M}_y(s) = M_{yo}/s$, and the response functions (19.49) become

$$\Theta = \frac{M_{yo}/J_y}{s(s^2+\omega^2)} \qquad \Psi = \sqrt{\frac{J_y}{J_Z}}\,\frac{(M_{yo}/J_y)\omega}{s^2(s^2+\omega^2)} \tag{19.53}$$

The corresponding time response is

$$\boxed{\theta(t) = \frac{M_{yo}}{J_y\omega^2}(1-\cos\omega t)u(t) \qquad \psi(t) = \frac{M_{yo}}{h}\left(t - \frac{\sin\omega t}{\omega}\right)u(t)} \tag{19.54}$$

[In the expression for $\psi(t)$, ω has been replaced by $h/\sqrt{J_yJ_Z}$.] Figure 19.12*a* shows this response, plotted in the manner of Fig. 19.11. The path made by the spin axis is called a cycloid. (It is the pattern traced by a point on the rim of a rolling wheel, as is readily shown.) The steady part, $\psi(t)_{\text{steady}} = (M_{yo}/h)t$ is called *precession* of the gyro, and the nodding up and down that is superposed on it is called *nutation*. The precession $\psi(t)$ is steady about an axis perpendicular to the axis about which the torque is applied, which is somewhat spectacular the first time it is experienced.† For the no-damping model assumed (which is closely approximated by many real

† An easy demonstration is to spin up a free bicycle wheel, for example, and then try to rotate it about a diameter. Motion (19.54) can be obtained with the bicycle wheel by hanging it from a string fastened to one end of its axle. Gravity furnishes $M_y(t)$. (The sinusoidal part of the motion is quickly damped.)

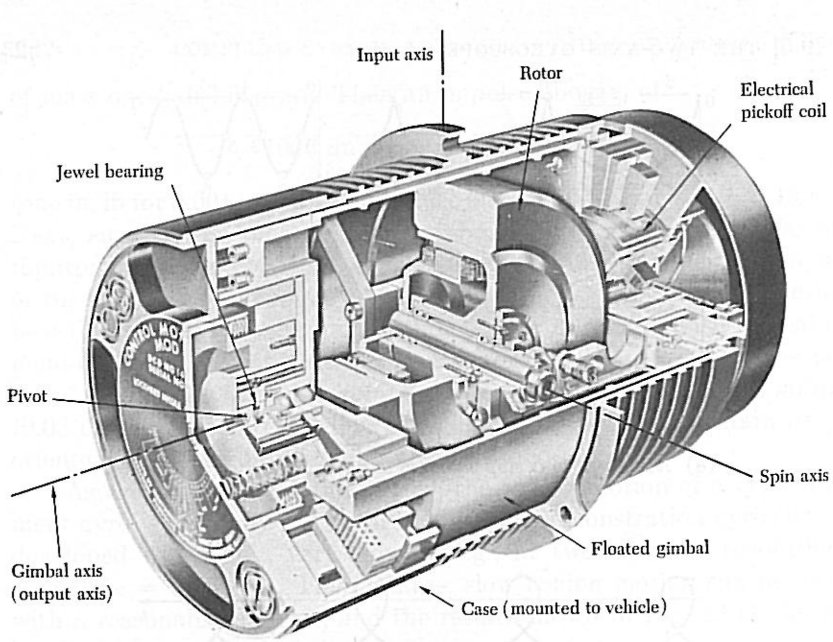

(*a*) *Floated, single-axis gyro (Courtesy Northrop Nortronics, Inc.)*

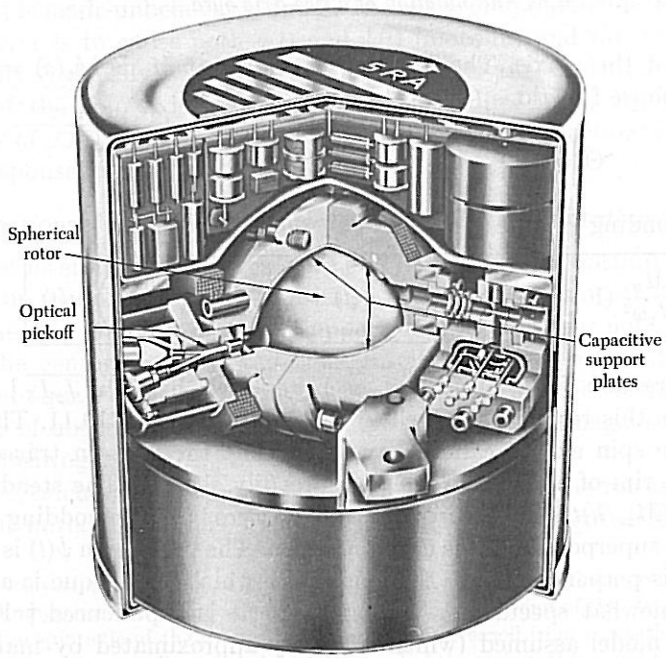

(*b*) *Spherical rotor supported electrically in a vacuum (Courtesy Honeywell, Inc.)*

Fig. 19.13 *Low-friction gyro designs*

gyros) the gyro may precess around in a complete circle many times, nodding (nutating) all the way.

As with the gyro's impulse response, shown in Fig. 19.11 (which is also commonly referred to as "nutation"), the response of Fig. 19.12*a* is large enough to observe only in a very slowly spinning gyro having large unbalance. Other fascinating patterns such as that in Fig. 19.12*b* can be created by superposing some of the motion of Fig. 19.11 on that of Fig. 19.12*a*, by applying an impulse after the motion of Fig. 19.12*a* has been started, for example.

The presence of damping causes the nutation motion to decay away eventually, and also results in precession with a small vertical component (the spin axis drops slowly). See Problem 19.30.

Precession

In the design of instrument gyros the crucial quantity is steady-state gyro precession. From (19.54) and Fig. 19.12*a* (lower plot) this is given by

$$\text{\textit{Gyro drift}} \qquad \boxed{\dot{\psi}(t) = \frac{M_{yo}}{h}} \tag{19.55}$$

or, in vector form,

$$\mathbf{\Omega} \times \mathbf{h} = \mathbf{M} \tag{19.56}$$

where $\mathbf{\Omega} = \mathbf{1}_Z\dot{\psi}$, $\mathbf{h} = \mathbf{1}_x h$, $\mathbf{M} = \mathbf{1}_y M_{yo}$, the precession being about an axis perpendicular to the axis of the applied torque. This is sometimes referred to as "the law of the gyro." Indeed, in most instrument gyros h is very large and there is some damping, so that the coning motions are tiny and short-lived. Then the steady precession (19.55) makes itself known over a period of time, and its magnitude determines the worth of the gyro as an inertial reference. But, as we have shown, there is much more to the dynamic behavior of a gyro than (19.55) foretells.

The accuracy of gyros

Gyroscopes, both free and single-axis, may be classified by random drift rates into three broad groups. Gyros used to stabilize short-range missiles, torpedoes, and fire-control antennas have random drift rates measured in degrees per minute. The free gyros used for attitude reference in aircraft have typical unsupervised drifts measured in degrees per hour. The gyros used to stabilize inertial navigation equipment must be made to have drifts measured in degrees per year.

Gyro drift can be controlled only by extremely careful balancing, by reducing bearing friction to the smallest possible value, and by preventing temperature and magnetic effects from causing drift-producing torques. Control of these effects has been the subject of extensive fundamental research.

An important factor in reducing the drift of gimbaled gyros is the prevalent use of the floatation technique, whereby the friction level in the gimbal bearings is greatly reduced. A typical construction is illustrated in Fig. 19.13*a* for a single-axis (single-gimbal) gyro. The gimbal is a sealed float which houses the rotor. The float is suspended in a liquid whose density is just sufficient to relieve the gimbal bearings of the rotor weight; therefore, friction at these bearings is greatly reduced—perhaps by a factor of 1000. Floatation may also be used with two-gimbal gyros.

An alternative technique is to use gas for support, either of a cylindrical gimbal like that in Fig. 19.13*a*, or of a spherical free rotor in a cup-shaped bearing.

A more fundamental approach to the bearing-friction problem, and one that has led to the most accurate gyros yet produced, employs a spherical rotor suspended electrically or magnetically in an extremely good vacuum, as in Fig. 19.13*b*, which shows an electrical suspension. Support is effected by controlling the plate voltages with position-feedback signals, as indicated in Fig. 2.27*f*. Location of the spin axis (corresponding to angles ψ and θ in Fig. 19.10*a*) is sensed optically.

As an extreme case, a research program at Stanford University includes plans to operate a spherical-rotor gyro having *no* support forces, by orbiting it in a special satellite controlled to follow it without touching. The purpose is to measure two general relativity effects, and the design goal is a drift rate of about one degree per 100,000 years.†

Problems 19.1 through 19.30

† R. H. Cannon, Jr., "Requirements and Design for a Special Gyro for Measuring General Relativity Effects from an Astronomical Satellite," *Gyrodynamics*, H. Ziegler, ed., Springer Verlag, Berlin, 1963.